



Using Non-Sub sampled Shearlet Transform and Nakagami Model for Ultrasound Image De-Speckling

Sedigheh Ghofrani

Electrical and Electronic Engineering Department, Tehran South Branch, Islamic Azad University,
 Tehran, Iran

s_ghofrani@azad.ac.ir

Received: 2015/03/07; Accepted: 2015/08/16

Abstract

Ultrasound images suffer of multiplicative noise named speckle. Different de-speckling algorithms run either in spatial domain or in transformed domain. In this paper, an adaptive filter in spatial domain according to assume the Nakagami distribution as the statistic of log-compressed ultrasound images is used. For de-speckling in transformed domain, the non-sub sampled shearlet transform is used. In addition, the Bayesian shrinkage as a well-known method for finding the optimum threshold values in transformed domain is applied. The main contribution of this paper is comparing the performance of two methods that suppress the speckle noise in spatial domain and transformed domain. For this purpose, a synthetic test image and the original ultrasound images are processed and peak signal to noise ratio (PSNR), mean square error (MSE), structural similarity (SSIM), edge keeping index (EKF), noise variance (NV), mean square difference (MSD), and equivalent number of looks (ENL) are obtained.

Keywords: Nakagami distribution, adaptive filter, non sub-sampled shearlet transform, ultrasound image de-speckling, Bayesian shrinkage thresholding.

1. Introduction

Being non-invasive, low cost, portability and real time make ultrasound imaging an essential tool for medical diagnosis. Multiplicative speckle noise in ultrasound imaging is an undesirable interference effect occurring when two or more ultrasound waves interfere with each other, constructively or destructively, producing bright and dark spots [1]. Speckle degrades both the spatial and contrast resolution of any coherent imaging systems including ultrasound and thereby speckle suppression is necessary before processing like image segmentation, edge detection, and in general any medical diagnosis. De-speckling is not only directly relevant to ultrasound images but also relevant to synthetic aperture radar, optical laser and other image modalities [1]. A wide variety of methods have been proposed to address the speckle removal or reduction for a variety of applications. In general, there are two basic approaches for image de-noising; spatial domain methods and transformed domain methods [2].

In some spatial domain methods, the local statistical properties of speckle utilized [3]-[6]. The statistic of speckle formation for log-compressed B-scan images based on Nakagami distribution was derived in [7]. Subspace-based technique is another method for noise reduction in spatial domain [8]- [10]. The fundamental principle of subspace-based de-noising is to decompose the data matrix of the noisy image into signal and

noise subspaces. Image enhancement is achieved by nulling the noise subspace and estimating the clean image from the remaining signal subspace.

In general, modeling and thresholding are two most used methods for despeckling in transform domain. While some researchers try to find an appropriate probability density function to model the free of noise coefficients such as two-sided generalized Gamma distribution (GFD) [11] in non-subsampled Contourlet transform, two dimensional generalized autoregressive conditional heteroscedastic generalized Gaussian (2D-GARCH-GG) [12] in Wavelet transform, and heavy-tailed Levy distribution [13] in Wavelet transform, others put an effort to obtain the optimum threshold values in transformed domain [1]. Finding the optimum threshold value is based on the idea that the energy of the signal concentrates on some of the transformed coefficients, while the energy of noise spreads throughout all transformed coefficients. The threshold value can be obtained adaptive or non-adaptive per sub-band. Bayesian shrinkage [14] is the adaptive threshold method. Thresholding methods are particularly effective for sparse representations where most of image information is concentrated in few large coefficients [1].

Although, wavelet transform is the most well-known two dimensions and multi-resolution transform, researchers attempt to find new two dimensions and multi-resolution transforms with more directionality. Due to, shearlet transform [15]-[16] were proposed. Shearlet transform similar to continuous wavelet transform represents an affine system obtained by scaling and translation and in addition unlike wavelet transform it has an extra parameter called shear. The original shearlet transform because of using up- and down-sampling is shift variant. That means, the coefficients are changing whenever the original signal is translating. Recently, the non-subsampled shearlet transform (NSST) [17] was introduced by omitting the up- and down-sampling blocks. As the coefficients do not decimate between the decomposition levels, all sub-bands sizes are the same as the original input image. However, in some papers, the NSST were used [17], [18], [19].

In this paper, two filters that work in spatial domain based on Nakagami as an old distribution and in transform domain based on NSST as a new multidirectional and multiresolution transform are applied in order to enhance ultrasound images that inherently corrupted by multiplicative speckle noise. In NSST domain, we used Bayesian shrinkage to find the optimum threshold value for each decomposition level and each sub-band. The NSST has the property of high directionality, anisotropy and translation invariance, which can be controlled by non-subsampled filter banks. As the NSST is a new transform, few papers [18]- [19] used it for ultrasound image de-noising. According to the experimental results (visual evaluation and some image assessment parameters) using the adaptive filter based on Nakagami distribution is preferred due to easy implementation and appropriate performance. It is the main achievement of this paper.

The paper is organized as follows. In Section 2, the statistic for log-compressed ultrasound images based on Nakagami model and accordingly the adaptive speckle suppression filter are explained. The speckle de-noising in transform domain by Bayesian shrinkage thresholding is explained in Section 3. The experimental results for adaptive filter based on Nakagami distribution and Bayesian shrinkage based on NSST are given in Section 4. In addition, the performance of spatial domain and transformed domain methods are compared according to some image assessment parameters. Finally, we have conclusion in Section 5.

2. Adaptive Filtering Based on Nakagami Distribution

In ultrasound imaging, the statistic of the echo envelope is followed by different distribution functions such as Rayleigh [20] and K [6]. Nakagami model was proposed in wireless communication and then used in ultrasound images [7], [21]. The model is given as,

$$P(A) = \frac{2m^m A^{2m-1}}{\Gamma(m)\Omega^m} \exp\left(-\frac{mA^2}{\Omega}\right) \tag{1}$$

Where $A \geq 0$ is the envelope amplitude, $\Gamma(.)$ is the gamma function, $m > 0.5$ the Nakagami parameter $m = (E(A^2))^2 / E(A^2 - \bar{A}^2)^2$ and $\Omega = E(A^2)$. Clinical ultrasound imaging systems use logarithm function to reduce the dynamic range of the input echo signal and emphasize objects with weak back scatter. In compression operation the following equation is used:

$$X = D \ln(A) + G \tag{2}$$

Where A is the input and X is the compressed output signal, D is the compression parameter and G is the linear gain. A is supposed as a Nakagami random variable then the variance, $VAR(X)$, of log-compressed signal is [7],

$$VAR(X) = \frac{D^2}{4} \zeta(m) \tag{3}$$

Where $\zeta(m) = \sum_{k=1}^{\infty} 1/(m+k)^2$? Equation (3) shows that the variance of the log-compressed envelope become smaller as the scatter becomes larger, in [7], the parameter \hat{f}_m was defined,

$$\hat{f}_m = \frac{\hat{D}^2 / 4}{VAR} \tag{4}$$

Where \hat{D} the estimated dynamic range parameter and VAR is is the local variance. The range of \hat{f}_m is limited to [0 , 1]. It means that any larger value is truncated to one. By defining the control parameter, $k = 1 - \hat{f}_m$, an adaptive filter [7] is,

$$\hat{X} = \bar{X} + k(X - \bar{X}) \tag{5}$$

Where \bar{X} is the local mean? The control parameter k varies adaptively between [0, 1]. Hence the filter output will range from maximal smoothing to no filtering.

3. Bayes Shrink Thresholding

As mentioned before, thresholding is basically an approach for de-speckling in transform domain. The main problem in thresholding method is finding the optimum threshold value [1]. This threshold can be adaptive or non-adaptive per sub-band. In

transform domain, Y_i , X_i and N_i are represented as noisy signal coefficient, noise free signal coefficient and noise component coefficient for any coefficient indexed by i . Then, for any linear transform, we have

$$Y_i = X_i + N_i \quad (6)$$

In this paper, in order to estimate coefficient \hat{Y}_i based on the observed coefficient Y_i , soft thresholding is used,

$$\hat{Y}_i = \begin{cases} 0 & |Y_i| < \lambda \\ \text{sign}(Y_i) \cdot (|Y_i| - \lambda) & |Y_i| \geq \lambda \end{cases} \quad (7)$$

According to Eq. (7), the soft thresholding involves first setting to zero the elements whose absolute values are lower than the threshold then scaling the nonzero coefficients toward zero [1].

The Bayesian shrinkage or Bayes Shrink [14] computes the optimum threshold values at each decomposition level and for every sub-bands separately,

$$\lambda_{l,k} = \frac{(\sigma_N^2)_{l,k}}{(\sigma_X)_{l,k}} \quad (8)$$

Where $\lambda_{l,k}$ is Bayes Shrink threshold, $(\sigma_N^2)_{l,k}$ is noise variance and $(\sigma_X)_{l,k}$ is the standard deviation of the noise free signal for any level ' l ' and sub-band ' k '. For implementing the Bayes Shrink in transform domain based on (8), the noise variance and the free noise signal variance are to be estimated for each decomposition level and sub-band. To simplify the notation, in following, the subscripts l and k that indicate level and sub-band are dropped. In this work, in order to estimate the standard deviation of noise, σ_N , the robust median estimator is used,

$$\sigma_N = \frac{\text{median}(Y_l)}{0.6745} \quad (9)$$

Where Y_l denotes the transformed coefficient of finest scale sub-bands. Furthermore, assuming a linear transformation, it can be written $Y = X + N$ for each level and any sub-band. Assuming that the signal coefficients and the noise coefficients are also independent at each level and any sub-band [22], i.e. we have $\sigma_Y^2 = \sigma_X^2 + \sigma_N^2$ where σ_X^2 is the signal variance without noise and σ_Y^2 is the variance of noisy signal obtained as,

$$\sigma_Y^2 = \frac{1}{MN} \sum_{i=1}^M \sum_{j=1}^N Y_{i,j}^2 \quad (10)$$

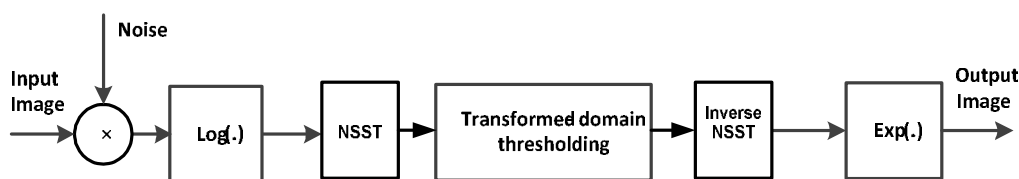


Figure 1. The block diagram of speckle denoising method that works in NSST domain.

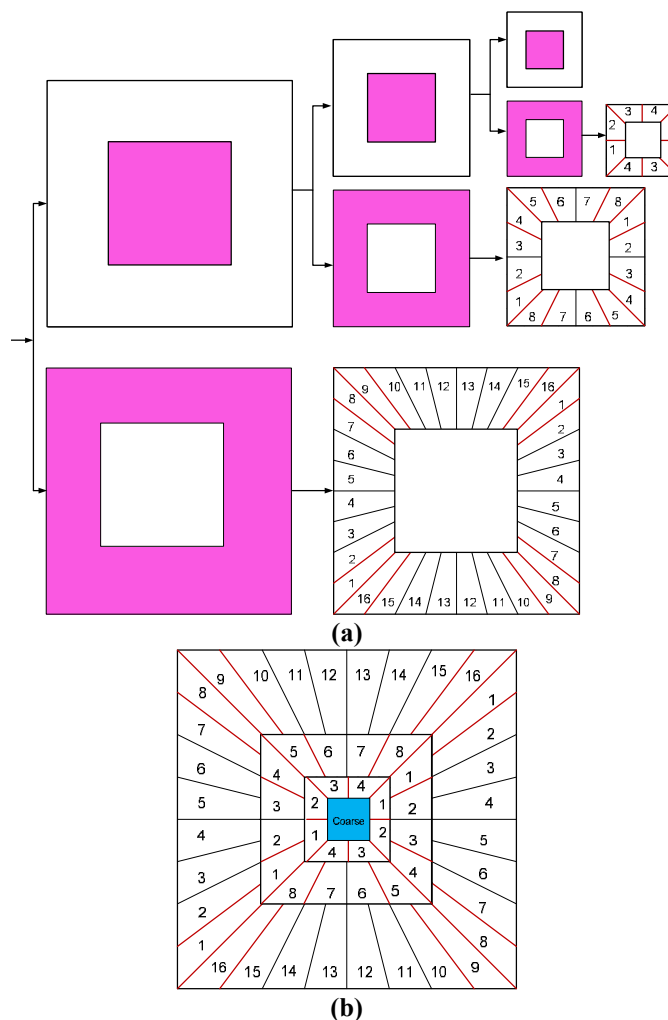


Figure 2. (a) The NSST of three levels decompositions, (b) the tilling frequency.

It was shown [22] that the variance of free noise signal can be estimated as,

$$\sigma_X^2 = \max(\sigma_Y^2 - \sigma_N^2, 0) \tag{11}$$

4. Experimental Results of De-Noising in Spatial and Transform Domains Based on Nakagami and NSST

For De-noising in spatial domain based on Nakagami distribution which named Adan-Nak, Eq. (5) is used where the parameter \hat{D} set 1.4, 1.6, 1.8 and the window size for computing the local mean and the local variance is 17×17 pixels.



Figure 3. Shown the Shepp-logan phantom image.

Table 1. Obtained the FR objective assessment parameters under different noise power in order to compare the performance of Ada-Nak for $D=1.4$ and BS-NSST. The Shepp-logan phantom image is used as the test image.

| | $\sigma^2 = 0.2$ | | | | $\sigma^2 = 0.4$ | | | | $\sigma^2 = 0.6$ | | | |
|-------------|------------------|-------------------------|------------------|----------------|------------------|--------------|--------|--------|------------------|--------------|--------|--------|
| | SSIM \uparrow | PSNR \uparrow (dB) | MSE \downarrow | EKI \uparrow | SSIM | PSNR (dB) | MSE | EKI | SSIM | PSNR (dB) | MSE | EKI |
| Noisy Image | 0.73 | 49.08 | 0.0074 | 0.5247 | 0.69 | 42.4 | 0.0144 | 0.3935 | 0.67 | 39.20 | 0.0198 | 0.3398 |
| Ada-Nak | 0.75 | 52.5 | 0.0052 | 0.5443 | 0.70 | 45.05 | 0.0111 | 0.3961 | 0.68 | 41.57 | 0.0156 | 0.3380 |
| BS-NSST | 0.73 | 49.68 | 0.007 | 0.5293 | 0.69 | 42.95 | 0.0136 | 0.3956 | 0.67 | 39.74 | 0.0188 | 0.3409 |

Thresholding methods are particularly effective for sparse representations where most of image information is concentrated in few large coefficients [1]. It was showed that the shearlet coefficients as a new multi-resolution transform belong to affine class are much sparse than the wavelet coefficients as the most well-known multi-resolution transform. So, in this paper, among many transform domains, the NSST is chosen and the optimum threshold is found based on Bayes Shrink. The proposed method named BS-NSST. In general, any filtering technique based on thresholding in transformed domain as shown in Figure 1 involves three steps: 1) computing the forward transform coefficients of a noisy image; 2) filtering the transform coefficients by means of thresholding; 3) reconstructing the clean or noise free image obtained by the inverse transform of filtered coefficients. An input image is decomposed into three levels by NSST. The decomposition levels, tilling frequency and the numbered sub-bands are shown in Figure 2. The noise variance for each decomposition level is obtained according to Eq. (9). For NSST, we have used sub-bands numbered 8, 16 and 4,8 and 2,3 in order for the first, second and third decomposition levels. The variance of noisy signal for all sub-bands based on Eq. (10) is computed and the variance of noise free signal according to Eq. (11) is estimated. The threshold value for each sub-band according to Eq. (8) is obtained, and the Bayesian soft thresholding for all sub-bands except the coarse one is applied. Finally the de-noising image is reconstructed by using the inverse transform.

In this paper for both approaches, Ada-Nak and BS-NSST (see Figure 1), the Homomorphic frame work (logarithmic transform at first and exponential transform at end) is used. Therefore, the multiplicative speckle noise model is converted to an additive one. All input images are normalized before using the logarithm transform.

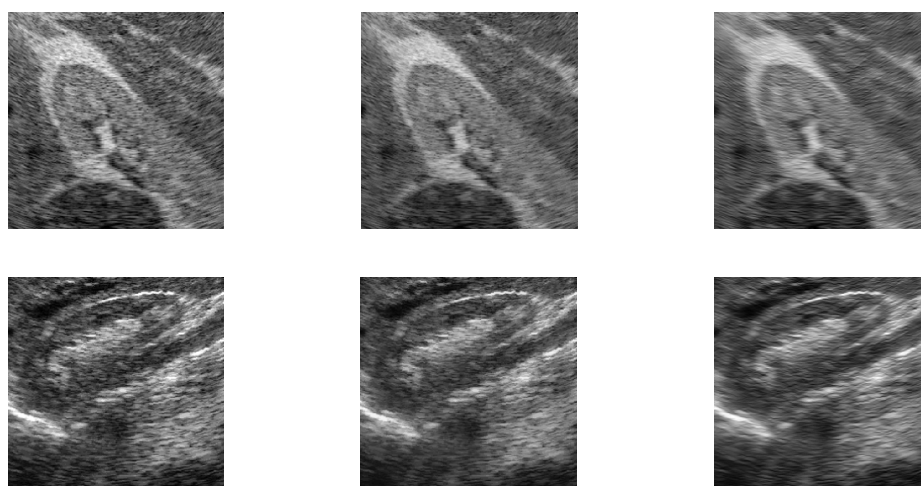


Figure 4. Shown the original ultrasound images (first column), the processing result for Ada-Nak for $D=1.4$ (second column), and BS-NSST (third column).

Table 2. The NR objective assessment parameters for two ultrasound images shown in Figure 4 in order to compare the performance of Ada-Na and BS-NSST.

| | | Image#1 | | | Image#2 | | |
|-------------|-------|---------|--------|-------|---------|--------|--------|
| | | NV↓ | MSD↑ | ENL↑ | NV | MSD | ENL |
| Noisy Image | | 0.0243 | 0 | 15.47 | 0.0322 | 0 | 8.56 |
| Ada-Nak | D=1.4 | 0.0202 | 0.0006 | 25.50 | 0.0273 | 0.0006 | 13.03 |
| | D=1.6 | 0.0191 | 0.0010 | 30.68 | 0.0260 | 0.0010 | 15.15 |
| | D=1.8 | 0.0181 | 0.0017 | 38.76 | 0.0247 | 0.0016 | 18.23 |
| BS-NSST | | 0.0201 | 0.0015 | 25.92 | 0.0275 | 0.0014 | 12.574 |

The performance evaluation of filters is a basic issue. In other word, there is a compromise between noise suppression and image preserving. So, the general goal is proposing a method that de-speckles images and preserves edges. For this purpose, peak signal to noise ratio (PSNR), mean square error (MSE), structural similarity (SSIM), and edge keeping index (EKF) as the full-reference (FR) objective criteria parameters, noise variance (NV), mean square difference (MSD), and equivalent number of looks (ENL) as the no-reference (NR) objective criteria parameters are used. Although PSNR is commonly used measures to quantify the noise suppression quality of the filtered image, it does not reflect the edge or structure preservation performance of the de-noising methods. Thus for the qualitative evaluations of structure and edge preservation in the filtered images, SSIM and EKI are used [19].

For any input image I_x and de-speckled image \hat{I}_x , in spatial domain, the image edge preservation parameter is,

$$EKF = \frac{\Gamma(\Delta_{I_x} - \bar{\Delta}_{I_x}, \hat{\Delta}_{I_x} - \bar{\hat{\Delta}}_{I_x})}{\sqrt{\Gamma(\Delta_{I_x} - \bar{\Delta}_{I_x}, \Delta_{I_x} - \bar{\Delta}_{I_x})\Gamma(\hat{\Delta}_{I_x} - \bar{\hat{\Delta}}_{I_x}, \hat{\Delta}_{I_x} - \bar{\hat{\Delta}}_{I_x})}} \quad (12)$$

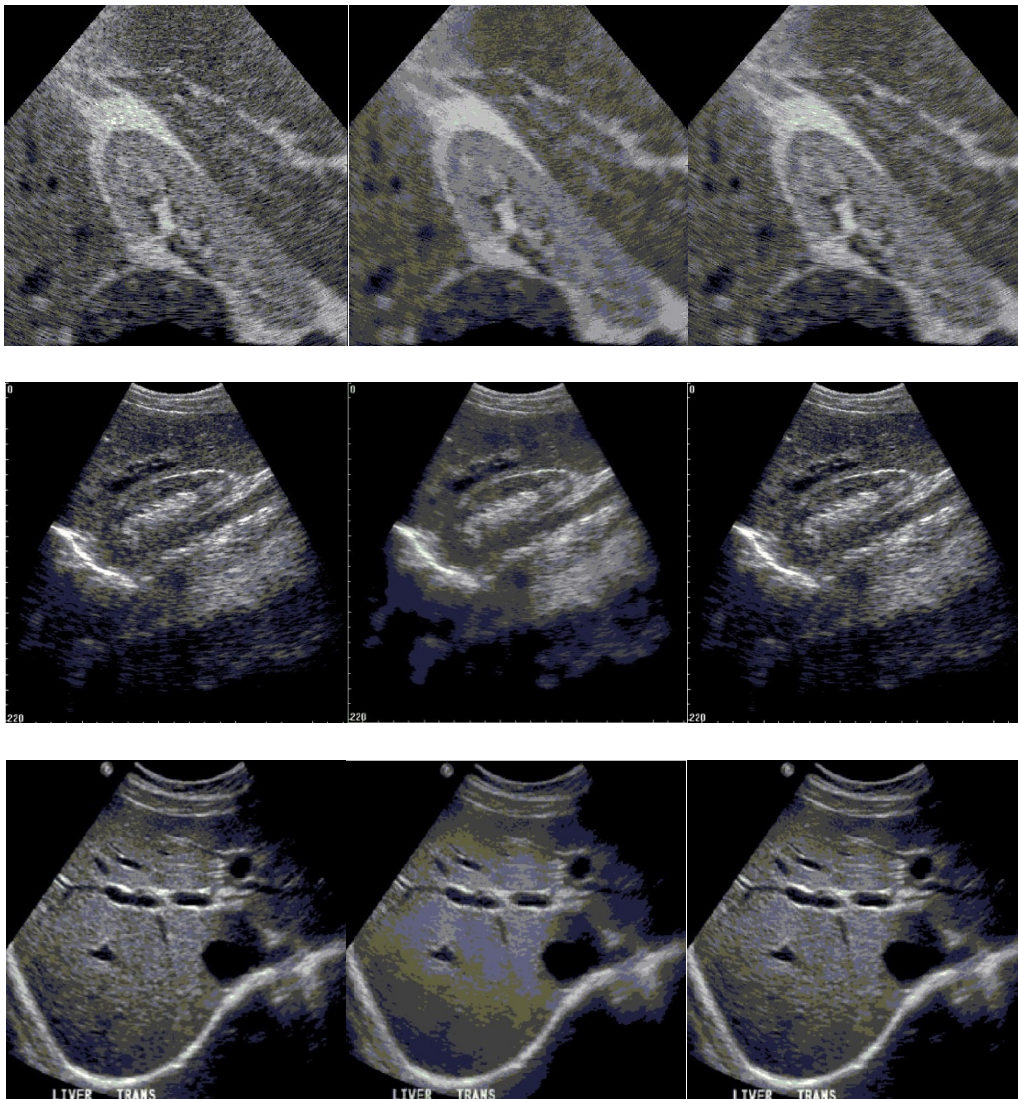


Figure 5. Three original ultrasound images (first column), the processed images by Ada-Nak for $D=1.8$ (second column), and BS-NSST (third column).

where $\Gamma(I_1, I_2) = \sum_{i=1}^M \sum_{j=1}^N I_1(i, j) I_2(i, j)$, $M \times N$ is the size of the image, Δ_{I_x} and $\hat{\Delta}_{I_x}$ are the high pass filtered version of $I_x(i, j)$ and $\hat{I}_x(i, j)$ obtained with 3×3 -pixel standard approximation of the Laplacian operator, the over line operator ($\overline{\Delta}_{I_x}$ and $\overline{\hat{\Delta}}_{I_x}$) represent the mean value. The correlation measures of (12) should be high, i.e., close to unity when the estimated image is similar to the reference image.

The second NR metric in spatial domain, NV, is

$$NV = \frac{\sum_{i=1}^M \sum_{j=1}^N [\hat{I}_x(i, j) - \overline{\hat{I}_x}]^2}{MN} \quad (13)$$

Where \bar{I}_x is the average intensity value of de-speckled image and obtained as $\bar{I}_x = \frac{1}{MN} \sum_{i=1}^M \sum_{j=1}^N \hat{I}_x(i, j)$, and MN refers to the image size. In general NV determines the contents of speckle in an image. It means, a lower variance gives a “smoother and cleaner” image. Another NR objective parameter, MSD, is

$$MSD = \frac{\sum_{i=1}^M \sum_{j=1}^N [\hat{I}_x(i, j) - I_y(i, j)]^2}{MN} \quad (14)$$

where I_y is the original noisy image. Although, high MSD shows the significant filter performance, we should be careful about blurring edges. The last used NR objective assessment parameter is ENL,

$$ENL = \frac{\bar{I}_x}{NV} \quad (15)$$

ENL estimates the speckle noise level in an image over uniform regions. On the other words, getting great ENL value shows appropriate performance of an algorithm. As ENL value depends on the tested region size, for obtaining the ENL, we split an image into blocks with 25×25 pixels and obtain ENL for each block separately, then we compute the average ENL and write the result in Table 2.

In this section, the performance of Ada-Nak, and BS-NSST in terms of subjective and objective image assessment are evaluated. Performing experiments on images with various contents enables us to give a general conclusion. In addition, to evaluate the effect of different methods, it is necessary to have reference images (without noise or with low noise level), to compare them with the output filters. So, we used the Shepp–Logan phantom image as a model of a human head which is shown in Figure 3, synthesize the speckle noisy image and apply the two methods, the achieved results are written in Table 1. The image assessment parameters averaged from 10 independent trials for different variance of noise. For two methods, obviously, the quality is decreasing while the noise variance is increasing. As said before, ultrasound images are extremely affected by speckle noise which may cause error decision about a patient disease. For real ultrasound images, there is not a clean signal or noise free signal. In following, two real ultrasound images are chosen for processing, see Figure 4. The visual results are shown in Figure 4 and the computed NR image assessment parameters are given in Table 2. Two arrow keys, “↑”, “↓”, for the FR and NR parameters in Table 1 and Table 2 are shown. The two arrow keys indicate either the maximum value or the minimum value is appropriate. Accordingly and unexpectedly, the spatial filtering based on Nakagami distribution outperforms the transformed filtering based on NSST. At the end, three original ultrasound images are de-speckled where the results for visual evaluation are shown in Figure 5. Although in [18], it was shown that the BS-NSST image denoising method enjoy superior performance in terms of both subjective and objective evaluation over wavelet and contourlet transforms for synthetic test images, in this paper for different cases, the Ada-Nak outperforms and because of less computation it is

preferred. Obviously, an appropriate method removes more speckle noise and has less blurring effects.

5. Conclusion

In this paper, two filters named Ada-Nak and BS-NSST that work in spatial domain based on Nakagami as an old distribution and in transform domain based on NSST as a new multidirectional and multiresolution transform are applied in order to enhance ultrasound images that inherently corrupted by multiplicative speckle noise and a test image as well. For implementing both methods, the statistical local information either in spatial or in transform domain is needed. In general, the main goal was finding a method that suppresses the speckle noise and preserves the image details as well. Unexpectedly, according to the experimental results (visual evaluation and some image assessment parameters) using the adaptive filter based on Nakagami distribution is preferred due to easy implementation and appropriate performance.

Acknowledgment

Sedigheh Ghofrani was supported in part by Islamic Azad University, Tehran South Branch. The title of project was, "Ultrasound Image De-speckling Based on Shearlet Transform".

References

- [1] G. Andria, F. Attivissimo, A. M. L. Lanzolla, and M. Savino, "A suitable threshold for speckle reduction in ultrasound images," *IEEE, Trans. On Instrumentation and Measurement*, vol. 62, no. 8, pp. 2270- 2279, 2013.
- [2] M. C. Motwani, M. C. Gadiya, R. C. Motwani, and F. C. Harris, "Survey of image denoising techniques," *Proceedings of Global Signal Processing Expo.*, pp. 27-30, 2004.
- [3] J.M. Park, W. J. Song and W. A. Pearlman, "Speckle filtering of SAR images based on adaptive windowing," *IEE, Vis Image Signal process*, vol. 146, no 4, pp. 191- 197, 1999.
- [4] P. M. Shankar, J. M. Reid, H. Ortega, C. W. Piccoli, and B. B. Goldberg, "Use of non-Rayleigh statistics for the identification of tumors in ultrasonic B-scans of the breast," *IEEE Trans. on Medical Imaging*, vol. 12, no 4, pp. 687- 692, 1993.
- [5] Chen, A. Zagzebski, "Non Gaussian versus non Rayleigh statistical properties of ultrasound echo signal," *IEEE Trans. on Ultrasonics, Ferroelect, Freq. Contr.*, vol. 41, no 4, pp. 435- 440, 1994.
- [6] P. C. Molthen, V. Manoj, Narayanan, P. M. Shakar, J. M. Reid, V. Genis and L. Vergara Domfnguez, "Ultrasound echo evaluation by K distribution," *IEEE Ultrasonics symposium*, vol. 2, pp. 957- 960, 1993.
- [7] S. Ghofrani, M. R. Jahed-Motlagh, and A. Ayatollahi, "An adaptive speckle suppression filter based on Nakagami distribution," *IEEE, International Cnference on Trend in communication*, vol. 1, pp. 84-87, 2001.
- [8] A. Zehtabian, and B. Zehtabian, "A novel noise reduction method based on subspace division," *Journal of Advances in Computer Research (JACR)*, vol. 1, no. 1, pp. 53- 59, 2010.
- [9] N. Yahya, N. S. Kamel, and A. S. Malik, "Subspace-based technique for speckle noise reduction in ultrasound images," *BioMedical Engineering On Line*, vol. 13, doi: 10.1186/1475-925X-13-154, 2014.

- [10] L. Hu, H. Ma, and L. Cheng, "Method of noise reduction based on SVD and its application in digital receiver front-end," IEEE, 18th Asia-Pacific Conference on Communications (APCC), pp. 511- 515, 2012.
- [11] M. Kiani, and S. Ghofrani, "Two new methods based on Contourlet transform for despeckling SAR images," SPIE, Journal of Applied Remote Sensing, vol.8, no. 1, pp. 083604 (1-13), doi:10.1117/1.JRS.8.083604, .2014.
- [12] M. Amirmazlaghani, and H. Amindavar, "Wavelet domain Bayesian processor for speckle removal in medical ultrasound images," IET, Image Processing, vol. 6, no. 5, pp. 580- 588, 2012.
- [13] J. J. Ranjani, and M. S. Chithra, "Bayesian denoising of ultrasound images using heavy-tailed Levy distribution," IET, Image Processing, vol. 9, no. 4, pp. 338- 345, 2013.
- [14] R. K. Rai, J. Asnani and T. R. Sontakke, "Review of shrinkage techniques for image denoising", International Journal of Computer Application, vol. 42, no. 19, pp. 13-16, 2012.
- [15] G. Easley, D. Labate, and W. Q. Lim, "Sparse directional image representations using the discrete shearlet transform," Elsevier, Applied and Computational Harmonic Analysis vol. 25, no. 1, pp. 25-46, 2008.
- [16] G. R. Easley, D. Labate, W. Q. Lim, "Optimally sparse image representations using shearlets," 40th Asilomar Conference on Signals, Systems and Computers, pp. 974- 978, 2006.
- [17] B. Hou, X. Z. Zhang, X. Bu, and H. Feng, "SAR image de-speckling based on nonsubsampling shearlet transform," IEEE, Journal of Selected Topics in Applied earth Observations and Remote Sensing, vol. 5, no. 3, pp. 809- 823, 2012.
- [18] S. Ghofrani, "Comparing nonsubsampling wavelet, contourlet and shearlet transforms for ultrasound image de-speckling," MECS, International Journal of Image, Graphics and Signal Processing, vol. 7, no. 2, pp. 15-22, 2015.
- [19] D. Gupta, R. S. Anand, B. Tyagi, "Speckle filtering of ultrasound images using a modified non-linear diffusion model in non-subsampling shearlet domain," IET, Image Processing, vol. 9, no. 2, pp. 107-117, 2015.
- [20] D. Kaplan, and Q. Ma, "On the statistical characteristics of log-compressed Rayleigh signals," IEEE, Ultrasonics symposium, vol. 2, pp. 961- 964, 1993.
- [21] P. Mohana Shankar, "A general statistical model for ultrasonic back scattering from tissues," IEEE Trans. On Ultrasonics, Ferroelect, Freq, Cont., vol 47, no 3, pp. 7270736, 2000.
- [22] D. X. Zhang, Q. W. Gao and X. P. Wu, "Bayesian-based speckle suppression for SAR image using Contourlet transform", Journal of electronic science and technology of china, vol. 6, no. 1, pp. 79-82, 2008.